American Journal of Pathology, Vol. 168, No. 4, April 2006

DOI: 10.2353/ajpath.2006.050607

Molecular Pathogenesis of Genetic and Inherited Diseases

The Ret^{C620R} Mutation Affects Renal and Enteric Development in a Mouse Model of Hirschsprung's Disease

Cristiana Carniti,* Sara Belluco,† Elena Riccardi,† Aaron N. Cranston,‡ Piera Mondellini,* Bruce A.J. Ponder,‡ Eugenio Scanziani,† Marco A. Pierotti,*§ and Italia Bongarzone*

From the Department of Experimental Oncology and Laboratories, Istituto Nazionale per lo Studio e la Cura dei Tumori, Milan, Italy; the Department of Animal Pathology,† Igiene e Sanità Pubblica Veterinaria–Sezione di Anatomia Patologica Veterinaria e Patologia Aviare, Università degli Studi di Milano, Milan, Italy; Institute of Molecular Oncology,§ Fondazione Italiana per la Ricerca sul Cancro, Milan, Italy; and the Department of Oncology,‡ the Cambridge Institute for Medical Research and Cancer Research United Kingdom, University of Cambridge, Cambridge, United Kingdom*

In rare families RET tyrosine kinase receptor substitutions located in exon 10 (especially at positions 609, 618, and 620) can concomitantly cause the MEN 2A (multiple endocrine neoplasia type 2A) or FMTC (familial medullary thyroid carcinoma) cancer syndromes, and Hirschsprung's disease (HSCR). No animal model mimicking the co-existence of the MEN 2 pathology and HSCR is available, and the association of these activating mutations with a developmental defect still represents an unresolved problem. The aim of this work was to investigate the significance of the RET^{C620R} substitution in the pathogenesis of both gain- and loss-of-function RET-associated diseases. We report the generation of a line of mice carrying the C620R mutation in the *Ret* gene. Although Ret^{C620R} homozygotes display severe defects in kidney organogenesis and enteric nervous system development leading to perinatal lethality. Ret^{C620R} heterozygotes recapitulate features characteristic of HSCR including hypoganglionosis of the gastrointestinal tract. Surprisingly, heterozygotes do not show any defects in the thyroid that might be attributable to a gain-of-function mutation. The *Ret*^{C620R} allele is responsible for HSCR and affects the development of kidneys and the enteric nervous system (ENS). These mice represent an interesting model for studying new therapeutic approaches for the treatment of HSCR disease. ***(Am J Pathol 2006, 168:1262–1275; DOI: 10.2353/ajpath.2006.050607)***

The *RET* proto-oncogene encodes a receptor tyrosine kinase (RTK) that is expressed widely in mammalian embryos and has diverse roles in development and disease.[1–5] In humans, heterozygous loss-of-function mutations of *RET* lead to the absence of enteric ganglia from the distal colon, characteristic of Hirschsprung's disease (HSCR).[6] In mice, a kinase-deficient Ret mutant is recessive and the mice lacked all enteric ganglia posterior to the stomach leading to intestinal aganglionosis, renal agenesis, and a defect in the superior cervical ganglia.[7,8] During embryogenesis, the main sites of RET expression are the excretory and nervous systems.[9,10] RET is also expressed in other derivatives of the neural crest including the C-cells of the thyroid and chromaffin cells of the adrenal gland.[9,10] Several of these tissues are affected in a dominantly inherited cancer syndrome called multiple endocrine neoplasia type 2 (MEN 2), which is caused by mutations in the *RET* gene. The MEN 2 cancer syndrome is usually divided into three different clinical subtypes: MEN 2A, MEN 2B, and familial medullary thyroid carcinoma (FMTC). The MEN 2A subtype is characterized by medullary thyroid carcinoma (MTC), pheochromocytoma, and parathyroid hyperplasia[11,12] whereas MTC, pheochromocytoma, ganglioneuromas of the intestinal tract, and skeletal and ocular abnormalities characterize MEN 2B. MEN 2B is the most aggressive of the three subtypes, often displaying an earlier age of onset. MTC is the only feature of FMTC, and it usually develops at

Supported by the Telethon Foundation (grant E0993), the Italian Association for Cancer Research, and Cancer Research UK. B.A.J.P. is a Gibb Fellow of Cancer Research UK.

Accepted for publication December 14, 2005.

Address reprint requests to Cristiana Carniti, Ph.D., Department of Experimental Oncology and Laboratories, Istituto Nazionale per lo Studio e la Cura dei Tumori, Via G. Venezian 1, 20133 Milan, Italy. E-mail: cristiana.carniti@istitutotumori.mi.it.

a later stage of life.[12] The course of MTC in FMTC families is more benign and prognosis is good. In virtually all MEN 2A and in many FMTC cases, mutations affect the RET cysteine-rich extracellular domain, each converting a cysteine to another amino acid, at codons 609, 611, 618, 620 (exon 10),[11] or at codons 630 and 634 (exon 11).[12]

In rare families, MEN 2A/FMTC and HSCR co-segregate,[11,13,14] and affected individuals carry a single substitution at one of the four cysteines in the extracellular RET domain (codons 609, 611, 618, and 620). The biological reasons accounting for this double phenotype are still under investigation. These mutations result in uncontrolled cellular proliferation in endocrine tissues and, on the other hand, result in the lack of neural development in the enteric system.[14]

Although experimental data demonstrated that *RET* MEN 2A/HSCR mutations markedly decrease RET cell surface expression,[15,16] both transfection experiments and biochemical analyses have shown that these cysteine codon substitutions cause ligand-independent dimerization, receptor activation, and cellular transformation[15,17] similar to the C634R substitution most frequently found in MEN 2A patients.[18–20] Indeed, the occurrence of HSCR in many MEN 2A/FMTC pedigrees is difficult to reconcile with the presence of a gain-of-function mutation in *RET*.

In an attempt to create a mouse model of RET MEN 2A/HSCR that recapitulates all of the sequelae of the human disease, we targeted the mouse *c-Ret* locus by homologous recombination to generate a line of transgenic mice in which the C620R mutation was knocked-in to the endogenous Ret locus. Homozygous Ret^{C620R} mutant mice die early after birth and display kidney agenesis and aganglionosis of the gastrointestinal (GI) tracts. Heterozygous Ret^{C620R} mutant mice are viable but exhibit features of the human HSCR disease including hypoganglionosis of the GI tracts. Surprisingly, although the mice recapitulate the loss-of-function phenotypes well, no abnormalities in the thyroid relating to a gain-of-function mutation were observed.

Materials and Methods

Gene Targeting

A mouse *Ret* genomic clone was isolated by screening a mouse 129/Sv bacteriophage DNA library (129/Sv) using the *Ret* cDNA containing exon 10, encoding the cysteine 620, as a probe. A targeting vector was constructed using a 1.8-kb *Bam*HI-*Bam*HI 5′ fragment and a contiguous 4-kb *Bam*HI-*Sac*I 3′ fragment that contained exons 10 and 11 in pBluescript SK (Stratagene, La Jolla, CA). In a *Bgl*II site immediately downstream of exon 11 a loxP-flanked pGK/neo/TK selection cassette (a gift from T.H. Rabbitts, MRC Laboratory of Molecular Biology, Cambridge, UK) was inserted. Specific mutagenesis of exon 10 was performed using a mutagenic primer 5′-AAGAAATGCTTC**C**GCGAGCCAGAGGACAGCCAG-3′ (bold letter indicates the base change) and the GeneEditor (Promega, Madison, WI) site-directed mutagenesis kit. The diphtheria toxin a chain gene contained within the pKOselectDT plasmid (Stratagene; GenBank Accession no. K01722; Greenfield and colleagues[21]) was inserted into the 5′ *Rsr*II site, such that it was outside the 5′ region of homology. The targeting construct was linearized with *Not*I and was electroporated into CCB embryonic stem (ES) cells (a gift from M.J. Evans, Cardiff School of Biosciences, Cardiff, UK) derived from the 129S7 strain. ES cells were plated on mitomycin C-treated primary embryo feeder cells grown on gelatin, which were obtained from a Rosa26 × MF1 cross (and therefore G418-resistant), followed by selection in G418. Clones that appeared to have the targeted insertion according to the applied polymerase chain reaction (PCR) screening method (P1, 5′-aagctctctagtcgaggaat-3′ and P2, 5′-ggcctctgaaggactgaa-3′) were confirmed by Southern blotting. The DNA was digested with *Bam*HI and hybridized to a probe obtained by amplifying a fragment containing *Ret* exon 11 and therefore present in both the targeted and nontargeted clones (P3, 5′-acaggggggaggtggtacagt-3′ and P4, 5′-atgccgtatccaccatctgt-3′). Direct DNA sequencing was used to confirm that targeted clones carried the C620R mutation. In the targeted clones (RetC620R-neoTK/+ ES), the floxed selection cassette was excised *in vitro* using pCre-Pac (a gift from D.J. Winton, Cancer Research UK Department of Oncology, University of Cambridge, Cambridge, UK) according to Taniguchi and colleagues.[22] Cre-mediated excision of the selection cassette was determined by a PCR screen (P5, 5′-cagggcttcccaatcagtt-3′ and P6, 5′-ccgagtacatgtgtgcctgt-3′) and analysis confirmed positive by DNA sequencing. A targeted RetC620R$^{+/-}$ ES cell clone was subsequently expanded and microinjected into C57BL/6J blastocysts at the Gene Targeting Facility, Babraham Institute, Cambridge, UK, to give rise to chimeric mice, which were used to transmit the mutation through the germline. Genotypes of these animals were confirmed using a two-primer assay (P7, 5′-tgccgacattgttggaggaac-3′ and P8, 5′-cctggctgttcctctggct-3′). In this genotyping assay, a 120-bp amplification product is generated from the wild-type allele that, after digestion with the restriction enzyme *Bst*UI, is not cleaved. Conversely, after digestion with *Bst*UI, the targeted allele yields a fragment of 98 bp. These PCR restriction digest products were resolved by agarose gel electrophoresis. Animals harboring the targeted mutation were bred to C57BL/6J mice to generation N3 before intercrossing and therefore segregate C57BL/NJ and 129S7 alleles in the ratio of 7:1. The official ILAR nomenclature for this mouse line is C57BL/6JN3TgH(Ret620)Ac620, which has been abbreviated to B6N3Ac620 and hereafter referred to as Ret^{C620R}.

Animal Husbandry

Mice carrying the Ret^{C620R} mutation were maintained on this mixed genetic background by intercrossing. For timed matings, the day of the vaginal plug was considered to be 0.5 dpc. All animals were maintained in barrier

facilities and treated in accordance with best husbandry practice and under the respective governmental and legislative requirements. Ethical approval was attained for these studies.

Reverse Transcriptase (RT)-PCR

RNA isolated from brains of adult mice was used to generate first strand cDNA, and gene-specific primers

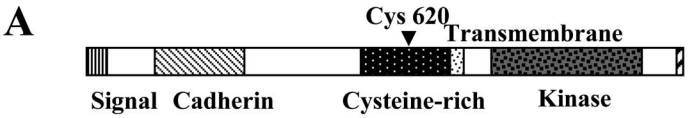

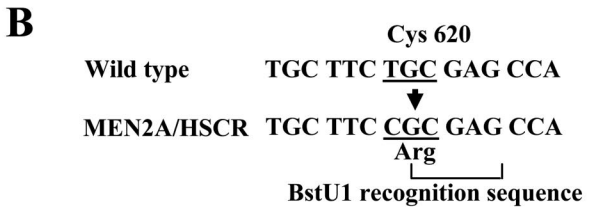

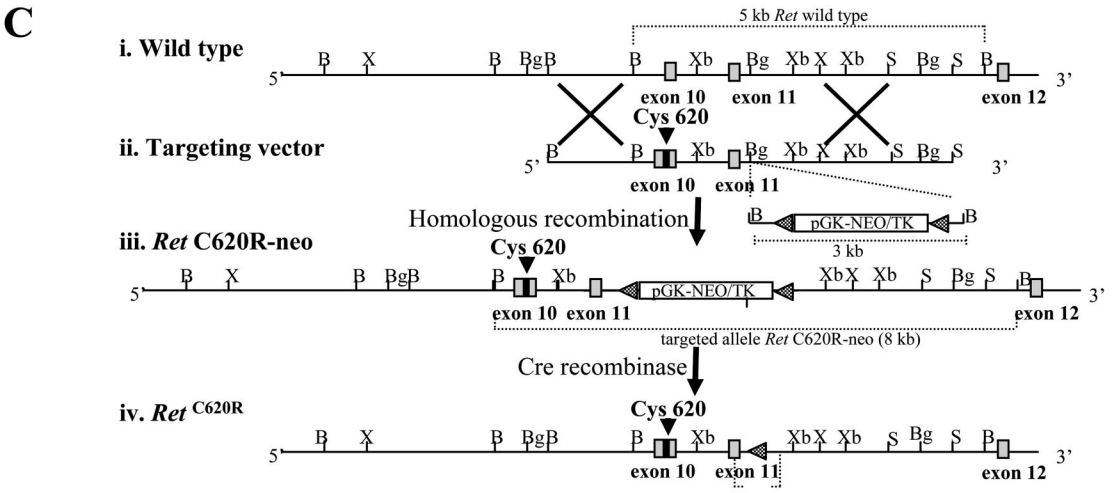

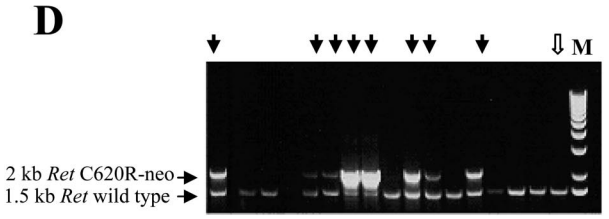

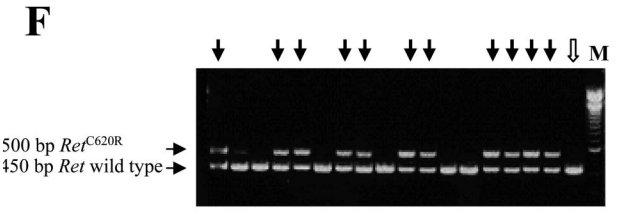

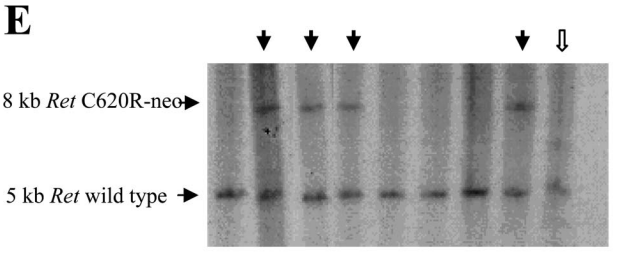

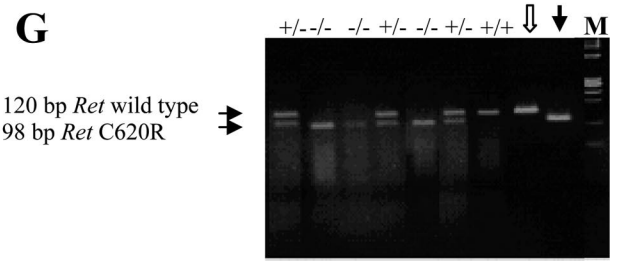

(P9, 5′-gtgccgacattgttgga-3′ and P10, 5′-tgcctgaggaggaataactgat-3′) were used to generate the amplification products of ~311 bp, which were then digested with *Bst*U1 to generate two fragments only when the targeted mutation is present. Primers for GAPDH were used as internal control of each reaction (P11, 5′-tgttcctaccccaatgtgt-3′ and P12, 5′-gtggaagagtgggagttgct-3′).

Immunoprecipitation and Western Blotting

Neonatal brains were homogenized in lysis buffer (2% Nonidet P-40, 40 mmol/L Tris-HCl (pH 7.5), 20 mmol/L ethylenediaminetetraacetic acid) supplemented with protease inhibitors (Complete Mini A; Roche, Basel, Switzerland), incubated on ice for 30 minutes and centrifuged at 4°C. Immunoprecipitation and Western blotting were performed according to standard procedures using protein A-Sepharose beads and a cocktail of monoclonal antibodies directed against the extracellular domain of RET (a generous gift of D.J. Anderson, Howard Hughes Medical Institute, California Institute of Technology, Pasadena, CA). Immunoblotting was done using a cocktail of polyclonal antibodies (Santa Cruz Biotechnologies, Santa Cruz, CA). As a control, proteins from mouse fibroblast NIH3T3 cells, which were transfected with pCEP9β plasmids containing either Ret^{C620R} and Ret^{C634R} as previously reported,[20] were extracted in lysis buffer, immunoprecipitated, and blotted as described above. For whole cell lysates, frozen tissues were homogenized in sodium dodecyl sulfate sample buffer containing 80 mmol/L dithiothreitol. The lysates containing 50 μg of protein were subjected to sodium dodecyl sulfate-polyacrylamide gel electrophoresis and Western blotting performed according to standard procedures using anti-vinculin (Sigma-Aldrich, St. Louis, MO), anti-Akt, anti-phospho-Akt, anti-Erk, and anti-phospho-Erk antibodies (Cell Signaling Technology, Beverly, MA).

Primary Culture of Dorsal Root Ganglia

Embryos were removed from the uterus of timed pregnant mice and placed in Petri dishes containing ice-cold phosphate-buffered saline (PBS). Dorsal root ganglia were obtained from 14.5 dpc embryos under a stereoscopic microscope and washed twice with ice-cold physiological saline and twice with Ham's F-12 (Gibco Invitrogen, Co., Carlsbad, CA). They were digested with 0.15% collagenase and 0.05% trypsin-ethylenediaminetetraacetic acid at 37°C for 5 minutes and mechanically triturated. Isolated cells were suspended in F-12 and 1.5 vol of Dulbecco's modified Eagle's medium supplemented with 10% fetal bovine serum (BioWhittaker, Walkersville, MD) were added. The cells were plated on 35-mm-diameter tissue culture dishes coated with filtrated 0.01% poly-L-lysine (Sigma) and maintained in a humidified incubator with 95% air and 5% CO_2 at 37°C. The medium was replaced with serum-free Dulbecco's modified Eagle's medium/F-12 (at a ratio of 1.5 to 1) 48 hours after the initial plating and kept for 24 hours until immunofluorescence analysis.

Immunofluorescence and Confocal Laser Microscopy

For primary cultures of DRG, cells were plated on 35-mm-diameter tissue culture dishes coated with filtrated 0.01% poly-L-lysine before immunofluorescence analysis with anti-RET antibodies. Cells were fixed in 4% paraformaldehyde and 2% sucrose and then permeabilized with 0.5% Triton X-100 in PBS. They were then subjected to indirect immunofluorescence with a cocktail of anti-RET polyclonal antibodies (H-300 and C-19, Santa Cruz Biotechnology). NIH3T3 fibroblasts were seeded at low confluence on glass coverslips and cultured for 24 hours. Cells were fixed in 4% paraformaldehyde and 2% sucrose and then permeabilized with 0.5% Triton X-100 in PBS. For surface labeling experiments, cells were incubated at 4°C with anti-RET rabbit-polyclonal antibodies raised against the N terminus of the protein (H-300, Santa Cruz Biotechnology) before cell fixation, permeabilization, and incubation with anti-RET goat polyclonal antibodies specific for the C terminus of RET (C-20, Santa Cruz Biotechnology). Immunostaining with primary antibod-

Figure 1. Introducing a MEN 2A/HSCR-associated mutation into the *Ret* locus. **A:** Structure of the normal protein encoded by the *Ret* gene. The location of the Cys620 is indicated. **B:** Site-directed mutagenesis to introduce the Cys620Arg mutation that generates a BstU1 recognition sequence (CGCG). **C:** Schematic representation of the targeting strategy. **i:** A fragment of the normal *Ret* gene including exons 10 to 12 (**gray boxes**). **ii:** The targeting vector includes a segment of genomic DNA containing exons 10 and 11. Exon 10 contains the mutation at position 620 so that the Cys in the Ret protein is replaced by an Arg. A selection cassette containing the neo gene flanked by two lox P sites has been inserted into the *Bgl*II site in the intron adjacent to exon 11. Lox P sites are indicated by **black triangles**. **iii:** Homologous recombination between the *Ret* genomic locus and the targeting construct introduced the mutant exon 10 and the loxP-neo-loxP gene in the intron adjacent to exon 11, to produce the RETC620R-neo allele. **iv:** The *Ret*^{C620R} allele was produced by Cre-mediated excision of the selection cassette. The restriction enzyme sites shown are B, *Bam*HI; Bg, *Bgl*II; S, *Sac*I; X, *Xho*I; and Xb, *Xba*I. **D:** PCR-based screening for the analysis of targeted ES cell clones. DNA extracted from G418-resistant ES cell clones was amplified by PCR (P1, 5′-aagctctctagtcgaggaat-3′ and P2, 5′-ggcctctgaaggactgaa-3′) to produce both a 2-kb fragment corresponding to the insertion in one allele of targeted clones (**black arrows**) and/or a 1.5-kb fragment in the wild-type ES cells (**white arrow**) and in the nontargeted clones. **E:** PCR results were confirmed by Southern blot analysis in which *Bam*HI-digested DNA was hybridized to a probe containing exon 11 and therefore present in both targeted and nontargeted clones. The probe was obtained by amplifying across the region using PCR (P3, 5′-acaggggaggtggtacagt-3′ and P4, 5′-atgccgtatccaccatctgt-3′). In this confirmatory screen the expected size of the targeted allele was 8 kb (**black arrows**), compared to 5 kb for the wild-type allele (**white arrow**). The position of the two alleles is indicated in C, **iii** and **i**, respectively. **F:** PCR-based analysis of targeted clones after Cre-mediated recombination. Targeted clones that had undergone Cre-mediated excision of the selection cassette displayed a band of the expected size (**black arrows**) after DNA amplification across the region of the inserted cassette. As a loxP site remains in the targeted allele this PCR amplification across the region (P5, 5′-cagggcttcccaatcagtt-3′ and P6, 5′-ccgagtacatgtgtgcctgt-3′) yields a band of ~500 bp, which is ~50 bp larger than the wild-type (**white arrow**) or nontargeted alleles. The location of the P5 and P6 primers is indicated in **C**, **iv**. **G:** PCR-based genotyping of tail biopsies from a representative litter of pups from a heterozygous breeding pair. A 120-bp amplification product (P7, 5′-tgccgacattgttggaggaac-3′ and P8, 5′-cctggctgttcctctggct-3′) was generated from the wild-type allele, which is not cleaved after digestion with the restriction enzyme *Bst*UI. Conversely, amplification and *Bst*UI digestion produced a product corresponding to 98 bp for the allele bearing the targeted C620R substitution. The products of the amplification and restriction enzyme digestion of wild-type DNA (**white arrow**) and DNA from the targeted Ret^{C620R} vector (**black arrow**) were loaded on the gel as internal controls. The genotype of each pup is indicated. +/+ wild-type; +/− heterozygous; −/− homozygous Ret^{620} mutant.

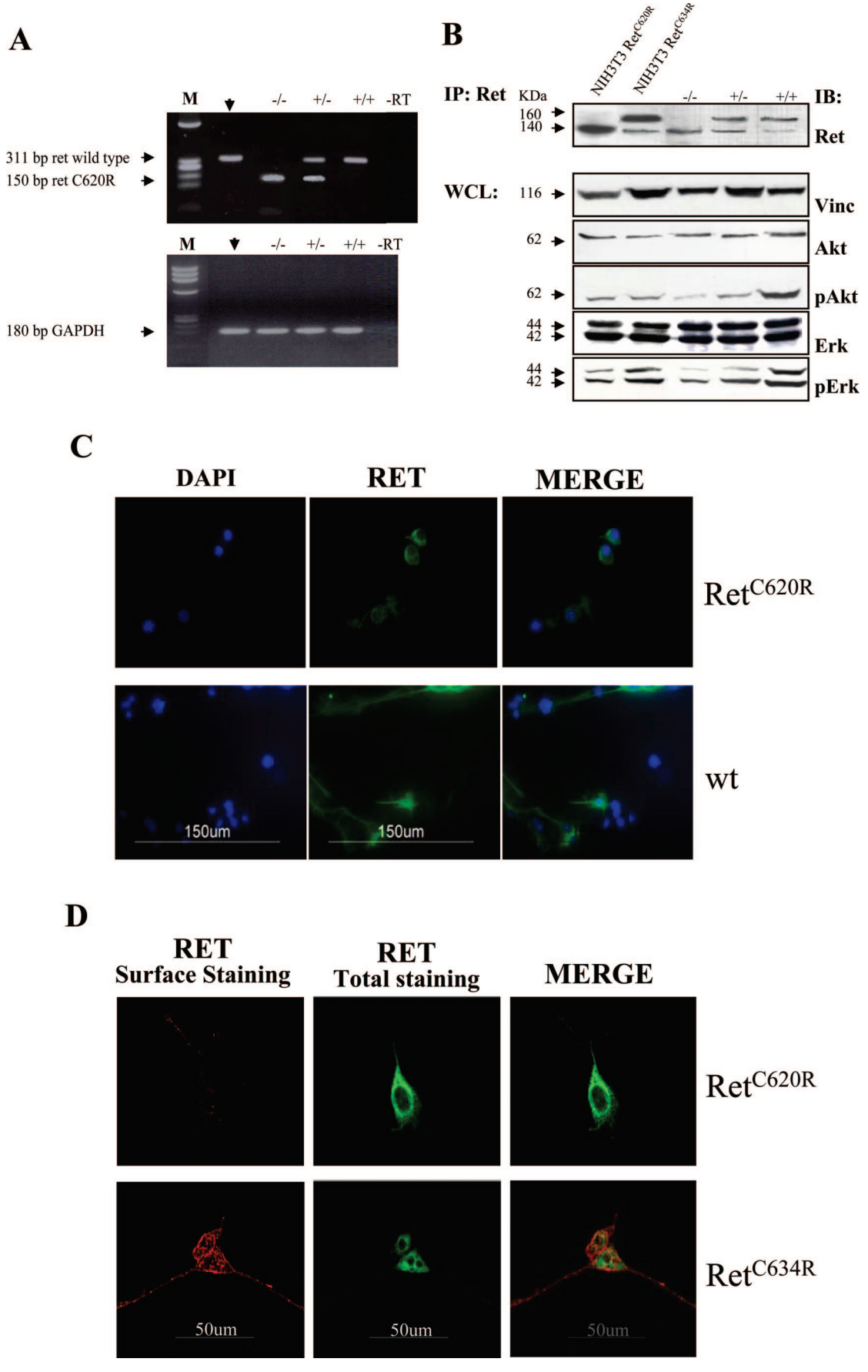
A
M
-/-
+/-
+/+
-RT
311 bp ret wild type
150 bp ret C620R
180 bp GAPDH
B
NIH3T3 RetC620R
NIH3T3 RetC634R
IP: Ret
KDa
IB:
160
140
Ret
WCL:
116
Vinc
62
Akt
pAkt
44
42
Erk
pErk
C
DAPI
RET
MERGE
RetC620R
wt
150um
D
RET
Surface Staining
RET
Total staining
MERGE
RetC620R
RetC634R
50um

ies was followed by incubation with rhodamine-conjugated AffiniPure donkey anti-goat IgG or fluorescein isothiocyanate-conjugated AffiniPure donkey anti-rabbit IgG from Jackson Immunoresearch (West Grove, PA). The confocal images were obtained using a Bio-Rad MRC-1024 confocal microscope.

Whole-Mount Immunostaining

For whole-mount immunostaining, embryos were dissected in PBS, fixed in 4% paraformaldehyde (in PBS) at 4°C for 1 to 2 hours. After two washes in PBS, they were incubated overnight in 0.1% H_2O_2 in PBT (PBS and 1% Triton X-100), washed again in PBT, and incubated for several hours in PBT containing 2 mg/ml bovine serum albumin and 10% goat serum. Incubation with anti-RET polyclonal antibodies (R787, IBL, Hamburg, Germany) was performed for 3 days at 4°C in PBT and 10% sheep serum. After extensive washes in PBT, the tissue was incubated with the polyclonal goat alkaline phosphatase-conjugated anti-rabbit immunoglobulins (DAKO Cytomation, Carpinteria, CA) for 12 to 16 hours and color development performed by incubating the embryos in BM Purple AP substrate (Roche).

Histological and Immunohistochemical Analysis

New born mice were killed by exposure to a rising concentration of CO_2 by inhalation, 1 hour after birth. They were fixed whole in 4% buffered formalin for 2 days after abdominal incision, and then decalcified in 10% ethylenediaminetetraacetic acid solution for 7 days. Each embryo was sectioned transversally in six parts, dehydrated in a graded ethanol series, and embedded in paraffin. Five-μm-thick transverse sections of the abdomen were taken every 250 μm and stained by hematoxylin and eosin (H&E) to evaluate the presence/absence of the kidneys as well as the morphology of each organ.

Adult animals of various ages were killed by cervical dislocation. The main organs of each mouse (heart, lung, thyroid, GI tract, liver, spleen, uterus, ovaries or testis, and kidneys) were collected, fixed in 10% buffered formalin, routinely processed for histological examination and paraffin-embedded. Transverse sections of small segments at defined locations along the GI tract were performed: the stomach was dissected from the cardias to the pyloric junction, the duodenum in the first part immediately below the pylorus, the jejunum in the middle of the tenue length, and the ileum immediately above the ileo-cecal junction. Both the apex and the body of the cecum and proximal and distal colon were collected. Immunohistochemistry with neuronal-specific enolase primary antibody (NSE, rabbit anti-human polyclonal antibody; DAKO) was performed on the sections. The number of ganglia and neurons in three ×400 fields was counted.

Digital Image Analysis

Histological sections were studied using a Jenaval research microscope (Zeiss, Jena, Germany) equipped with a video camera and connected to the image-analysis and morphometry system. Microphotographs were taken with a digital camera (Coolpix 990; Nikon, Tokyo, Japan). Three images for each of the GI segments described above were acquired at ×100 magnification. Morphometric analysis of the thickness of circular and longitudinal muscular layers was performed using Image-Pro Plus software according to the method described by J.M. Starck and G.H. Rahmaan.[23] At least five measurements of the muscular layer thickness were performed in each section and the mean value calculated.

Statistical Analysis

Student's *t*-test (two-tailed) was used to compare the number of neurons and the thickness of circular and longitudinal muscular layers in heterozygous and control

Figure 2. Expression of the RetC620R alleles. **A:** RT-PCR analysis of total RNA from neonatal brain. The 311-bp product specific for *R*et mRNAs is generated in each sample (P9, 5′-gtgccgacattgttgga-3′ and P10, 5′-tgcctgaggaggaataactgat-3′) but *Bst*U1 digestion gives rise to a cleaved fragment only in samples derived from animals carrying at least one copy of Ret^{C620R}. Amplification of *Gapdh* mRNA (P11, 5′-tgttcctacccccaatgtgt-3′ and P12, 5′-gtggaagagtgggagttgct-3′) verified the integrity of the mRNA. The product of the amplification and digestion of control wild-type RNA (**black arrow**) is loaded on the gel as a control. Genomic contamination was assayed by PCR omitting the reverse transcriptase (−RT). The genotypes of the animals used are shown: +/+, wild-type; +/−, heterozygous Ret^{C620R}; −/−, homozygous Ret^{C620R} mutant. **B:** Expression of the Ret protein and activation of Erk and Akt in Ret^{C620R} mice. Protein extracts from neonatal brain were immunoprecipitated and subjected to Western blot analysis using specific antibodies for Ret. Homozygous Ret^{C620R} mice (−/−) predominantly express the p140 band of Ret whereas heterozygous Ret^{C620R} mice (+/−) express comparable levels of both the p140 and p160 bands. Wild-type animals (+/+) mainly express the p160 band. As a control, proteins from NIH3T3 fibroblasts stably transfected to express Ret^{C620R} or Ret^{C634R} were immunoprecipitated and blotted with the same antibodies and loaded on the gel (for each genotype, $n = 10$). Whole cell lysates (WCLs) (50 μg) of neonatal brains of homozygous Ret^{C620R} mice (−/−), heterozygous Ret^{C620R} mice (+/−), and wild-type mice (+/+) were immunoblotted with anti-vinculin, anti-Akt, anti-phospho-Akt, anti-Erk, and anti-phospho-Erk antibodies. Immunoblotting with phospho-Erk and phospho-Akt antibodies highlighted that Erk and Akt activation is prevalent in wild-type (+/+) whereas weaker signals are detected in Ret^{C620R} heterozygous (+/−) and homozygous mice (−/−) although similar signals are present in Akt and Erk immunoblots for all of the mutants. To verify equal protein loading, anti-vinculin antibodies were used. As control, proteins from NIH3T3 fibroblasts stably transfected to express Ret^{C620R} or Ret^{C634R} were immunoblotted with the same antibodies, and loaded on the gel. **C:** Ret cellular localization in primary cultures of DRG. Cells from homozygous and wild-type animals were plated on 35-mm-diameter tissue culture dishes coated with filtrated 0.01% poly-L-lysine before immunofluorescence analysis with anti-RET antibodies. Cells were fixed in 4% paraformaldehyde and 2% sucrose and then permeabilized with 0.5% Triton X-100 in PBS. They were then subjected to indirect immunofluorescence with a cocktail of anti-RET polyclonal antibodies (H-300 and C-19, Santa Cruz Biotechnology). **D:** Ret^{C620R} cellular localization. NIH3T3 cell clones expressing Ret^{C620R} or Ret^{C634R} were examined by immunofluorescence confocal microscopy. For surface localization, cells were incubated at 4°C with an anti-RET antibody raised against the extracellular domain of the protein (H-300, Santa Cruz Biotechnology). They were then fixed, permeabilized, and stained with an antibody directed against RET carboxy-terminus to reveal the receptor intracellular distribution (C-20, Santa Cruz Biotechnology). Note that Ret^{C634R} mutant receptor but not Ret^{C620R} is localized at the cell surface, as revealed by surface staining obtained with the extracellular specific antibody (red staining). Staining with RET carboxy-terminus-specific antibody detects the presence of both mutant receptors in intracellular compartments (green staining). Scale bars: 150 μm (**C**); 50 μm (**D**).

wild-type mice. Results are expressed as the mean +/− SE of *n* observations. Statistical significance was determined by analysis of variance, where $P < 0.001$ was considered significant.

Results

Generation of RetC620R Knock-In Mice

To target the mouse Ret locus by homologous recombination in ES cells, codon 620 of murine *Ret*, the equivalent of human codon 620, was mutated *in vitro* to encode arginine rather than cysteine (Figure 1, A and B). A targeting vector was constructed to insert the mutant exon into the mouse genome along with a selection cassette (Figure 1C). After linearization, the targeting construct (Figure 1C) was electroporated into CCB ES cells isolated as described.[24] Four of one hundred clones had the targeted insertion according to the applied PCR screening method (Figure 1D). Southern blotting and direct DNA sequencing confirmed the presence of the targeted allele of the expected size and the presence of the C620R *Ret* mutation (Figure 1E and unpublished data). The selection cassette was removed after Cre-mediated excision according to Taniguchi and colleagues[22] as shown by PCR analysis performed on the DNA of the ES cell clones (Figure 1F). One targeted Ret C620R$^{+/-}$ ES cell clone was expanded and microinjected into C57BL/6J blastocysts to obtain chimeric mice. The chimera with the greatest ES cell contribution was chosen and used to transmit the mutation through the germline. The genotypes of these animals were confirmed using a two-primer assay: a 120-bp amplification product is generated from the wild-type allele that is not cleaved after digestion with the restriction enzyme *Bst*UI (CGCG), which would otherwise generate a 98-bp fragment for the allele bearing the C620R substitution (Figure 1, B and G). The whole *Ret* gene was sequenced to exclude the presence of other mutations apart from the C620R Ret mutation we had introduced (data not shown). Animals were bred to C57BL/6J mice to generation N3 before intercrossing and therefore segregate C57BL/6J and 129S7 alleles in the ratio of 7:1, respectively. The official nomenclature for this mouse line is C57BL/6JN3TgH(Ret620)Ac620, which has been abbreviated to B6N3Ac620 and hereafter referred to as Ret^{C620R}.

Characterization of the Ret^{C620R} Mice

To examine the products of the *Ret*^{C620R} alleles, RNA from embryos or newborn brain tissue was analyzed by RT-PCR using allele-specific primers and restriction enzyme analysis. As expected, homozygous Ret^{C620R} mice expressed only the *Ret*^{C620R} mRNA and lacked the wild-type *c-Ret* transcripts, whereas heterozygous animals expressed both the wild-type and the targeted allele (Figure 2A).

Using cell systems such as NIH3T3[15–17] or Madin-Darby canine kidney (MDCK) cells[25] in which diverse RET constructs have been introduced, different groups have demonstrated that the expression of the 160-kd isoform of RET bearing the Cys620 mutation was very low compared with that of wild-type RET, suggesting that this mutation impairs the transport of RET to the plasma membrane.[15–17] The 140-kd product is endoglycosidase H-sensitive, suggesting that the 140-kd band corresponds to an incompletely glycosylated precursor of RET present in the endoplasmic reticulum whereas the 160-kd band is the mature RET protein, fully glycosylated and expressed at the cell surface.[18,26] To analyze the products of the *Ret*^{C620R} alleles in our mouse model that represents a physiological system for the study of the effects of the RET^{C620R} mutation, protein extracts from embryos and newborn brain tissue of Ret^{C620R} homozygous, Ret^{C620R} heterozygous, or wild-type animals were immunoprecipitated with a cocktail of three different hamster anti-RET hybridoma supernatants (3A61D7, 3A61C6, and 2C42H1, kindly provided by D.J. Anderson) and the immunoprecipitates were characterized by Western blotting using specific antibodies for RET. In line with what was found in cell systems,[15–17,25] Western blot analysis in Ret^{C620R} homozygous mice showed the prevailing expression of the Ret 140-kd isoform. (Figure 2B). In contrast, wild-type mice showed almost exclusively the 160-kd isoform. As predicted by the genetic situation of Ret^{C620R} heterozygous mice in which just one *Ret*^{C620R} allele is present, the related brain protein extracts showed an expression pattern of Ret that included both the 160-kd and 140-kd isoforms (Figure 2B). Cell lysates prepared from NIH3T3 fibroblasts stably expressing comparable levels of either the Ret^{C620R} or the Ret^{C634R} mutant were used as controls in immunoprecipitation and Western blotting. In agreement with previous studies[15–17] the expression of the Ret^{C620R} mutants in fibroblasts was similar to the one detected in the homozygotes with the 140-kd isoform being the prevailing band present whereas the Ret^{C634R} mutant mainly expressed the 160-kd isoforms. Activation of Erk and Akt was assessed in the same tissues by immunoblotting. Staining with phospho-Erk and phospho-Akt antibodies highlighted that Erk and Akt activation is prevalent in wild-type mice whereas weaker signals are detectable in Ret^{C620R} heterozygous and homozygous mice suggesting that the Ret^{C620R} mutation can affect Erk and Akt signaling.

Given the expression of c-ret in all cranial ganglia and in dorsal root ganglia (DRG) in 13.5- to 14.5-day embryos[9] to try to assess the cellular localization of the Ret^{C620R} mutants, we performed primary DRG cell cultures from 14.5 dpc Ret^{C620R} homozygous, heterozygous, and wild-type mice that were examined for Ret positivity by immunofluorescence confocal microscopy. It was impossible to stain for the receptor at the surface of the living cells because the primary cultures tended to detach when incubated on ice with the anti-RET polyclonal antibody before fixation. Cells had to be fixed and were then subjected to indirect immunofluorescence with a cocktail of anti-RET polyclonal antibodies (H-300 and C-19, Santa Cruz Biotechnology) specific for RET extracellular and RET intracellular domains, respectively, and demonstrated to recognize both the

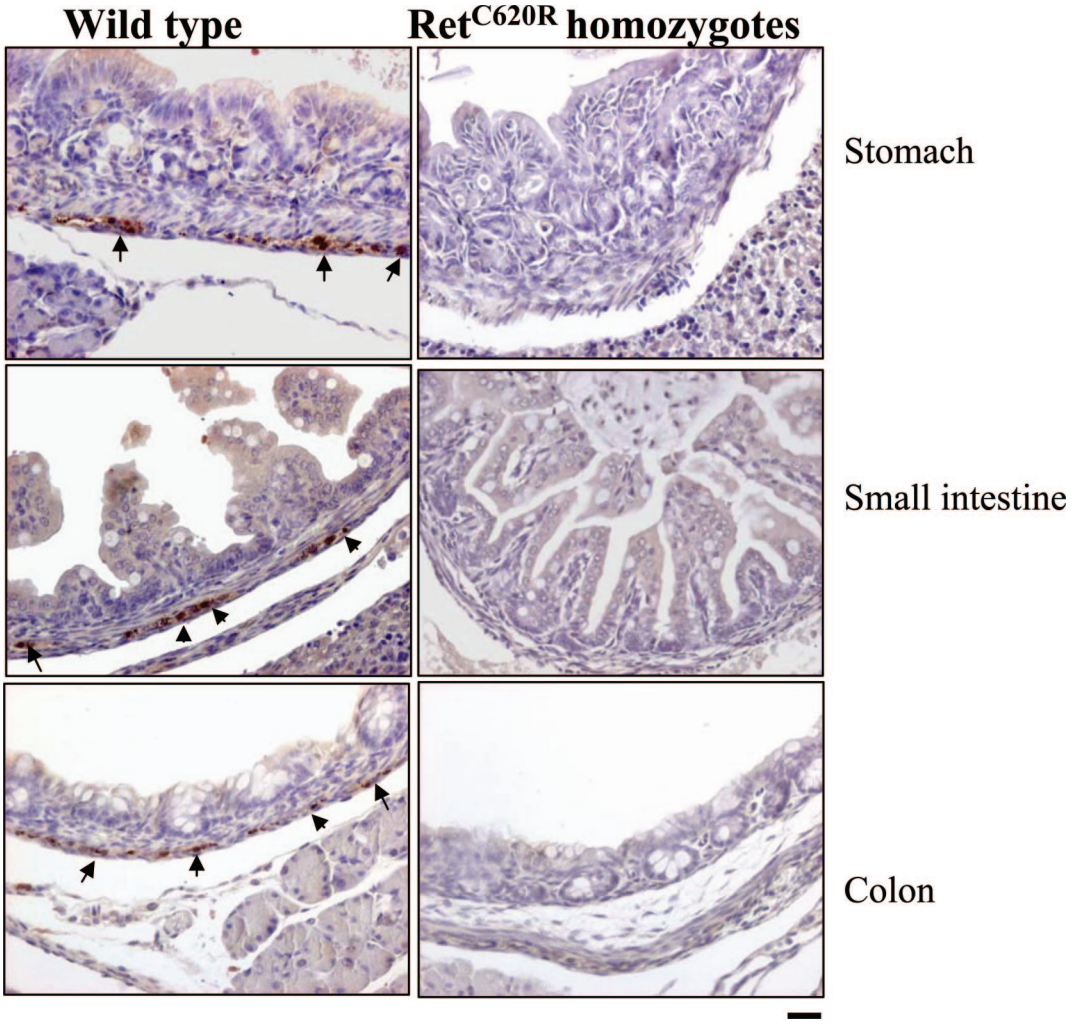

Figure 3. Immunohistochemical analysis of the enteric nervous system of Ret^{C620R} homozygous mice. Immunohistochemistry performed with antibodies specific for NSE identifies ganglion cells (**arrows**) in the wall of the GI tract of wild-type animals whereas no staining is present in Ret^{C620R} homozygous mice (for each genotype, $n = 5$). Scale bar, 50 μm.

mouse Ret wild-type and mouse Ret^{C620R} proteins in Western blotting experiments (data not shown). Few cells obtained from the primary cultures of 14.5 dpc Ret^{C620R} homozygous mouse brains expressed the receptor. In these cells, Ret seemed to be localized mainly intracellularly (Figure 2C) whereas for wild-type mouse cells (Figure 2C) and for Ret^{C620R} heterozygous mouse cells (data not shown), the antibody outlined the shape of the cells indicating a prevailing surface localization of the receptor (Figure 2C). Specificity of RET antibodies was ascertained by staining wild-type NIH3T3 cells, which lack Ret receptors, and NIH3T3 cells transfected with a Ret construct as described above (data not shown).

To further assess that the predominant presence of the 140-kd band reflected a decreased level of the Ret^{C620R} receptor present at the plasma membrane, NIH3T3 fibroblasts stably transfected to express either the Ret^{C620R} or Ret^{C634R} mutants, were examined by immunofluorescence confocal microscopy. The cells were incubated on ice with an anti-RET polyclonal antibody specific for RET extracellular domain (H-300, Santa Cruz Biotechnology) before fixation to stain for the receptor at the cell surface of the living cells. After fixation and permeabilization, cells were stained with the carboxy-terminus-specific antibody to reveal the receptor intracellular distribution (C-20, Santa Cruz Biotechnology). The carboxy-terminus-specific serum detected the presence of both the mutant receptors in intracellular compartments (Figure 2D, green staining). Signal was particularly intense in perinuclear regions suggesting a prevailing localization in the endoplasmic reticulum. Furthermore, the Ret^{C634R} mutant receptor but not the Ret^{C620R}, was localized at the cell surface, as revealed by surface staining obtained with the extracellular specific antibody in Figure 2D, red staining. Taken together these data indicate that even in these mice as it happens in cell transfection experiments, the *Ret*^{C620R} allele mainly encodes a p140 product, which corresponds to an intracellularly localized form of Ret present in the endoplasmic reticulum.[26] These findings therefore suggest that in our mouse model the Ret^{C620R} mutant receptor might lack from the plasma membrane of the RET-expressing cells.

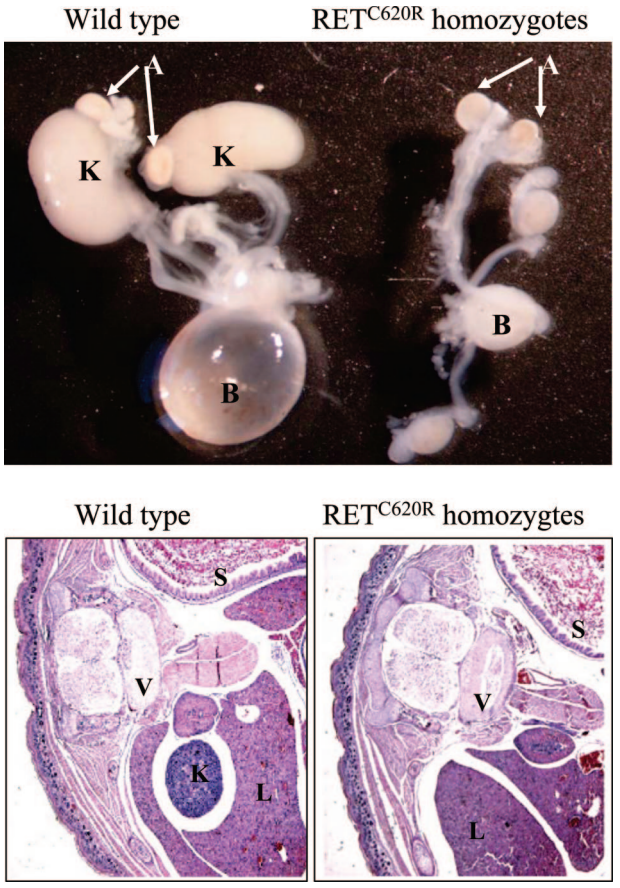

Figure 4. Kidney agenesis in Ret^{C620}R homozygous mice. Newborn mice, if they were not already dead, as in the case of the homozygotes, were killed by exposure to CO_2, 2 hours after birth. Macroscopic analysis revealed the absence of both the kidneys in Ret^{C620R} homozygous mice as well as empty bladder (**top**). Each embryo was sectioned transversally in six parts, dehydrated, and embedded in paraffin. Five-μm-thick transverse sections of the abdomen were taken and stained for H&E to further evaluate the presence/absence of the kidneys (**bottom**). Kidneys were absent in Ret^{C620R} homozygous mice. B, bladder; K, kidney; V, vertebral body; A, adrenal; L, liver; S, stomach (for each genotype, $n = 5$).

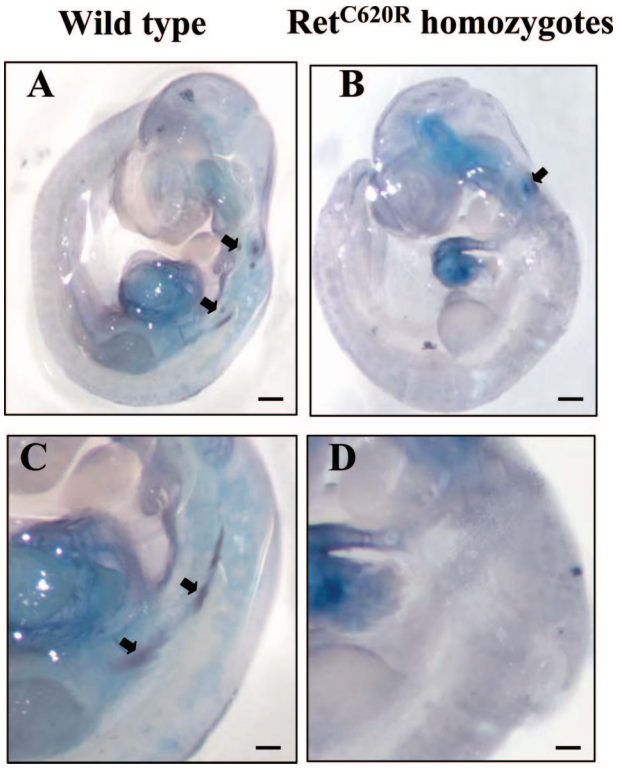

Figure 5. Expression of Ret in Ret^{C620R} homozygous mice detected by whole-mount immunostaining with an antibody specific for Ret. **A:** Whole-mount immunostaining showing the location of Ret expression. Lateral view of mouse embryo 10.5 days postcoitum (dpc) with strong expression in the developing peripheral nervous system. In wild-type animals, in the 10.5 dpc mouse embryo, a Ret-specific signal is observed in populations of cell (**arrows**) in the postbranchial region and in the developing foregut. **B:** In Ret^{C620R} homozygous embryos of the same age no Ret staining is visible in these areas whereas specific staining is observed probably corresponding to the fascioacoustic ganglion (**arrow**). **C:** In 11.5 dpc wild-type embryos, the same two populations of cells are present, the ventrally located one that will probably invade the foregut mesenchyme (**arrows**) and the more dorsal group in the postbranchial region proximal to the dorsal aorta (**arrows**), probably corresponding to ENS progenitors that will colonize the gut. **D:** In 11.5 dpc Ret^{C620R} homozygous embryos, no Ret staining is visible in these areas indicating that there are no Ret-positive cells contributing to the formation of the ENS (for each genotype and stage, $n = 5$). Scale bars, 400 μm.

Ret^{C620R} Homozygous Mice Die Soon after Birth

All heterozygous Ret^{C620R} mice appeared healthy, grew, and reproduced normally. The genotype distribution of the newborn mice obtained from Ret^{C620R} heterozygote intercrosses was as follows: wild-type 24%, heterozygous 51%, and homozygous 25%, indicating that there was no appreciable embryonic lethality of homozygous Ret^{C620R} mice. At birth, homozygous mutants were the same size as their wild-type and heterozygous littermates, responded to tail pinch, and nursed normally. However, all Ret^{C620R} homozygous mice died within 24 hours of birth as confirmed by genetic analysis performed on the DNA extracted from the mice tails.

Enteric Nervous System Deficits and Kidney Agenesis in Ret^{C620R} Homozygous Mice

Necropsy of postnatal homozygous Ret^{C620R} mice revealed that many of them had milk in the esophagus (which was not observed in wild-type animals) and little milk beyond the proximal small bowel, suggesting defects in GI peristalsis. Given the absence of enteric neurons beyond the stomach in Ret-, Gdnf-, and Gfrα-1-deficient animals, it seemed likely that these observations similarly reflected defects in the enteric nervous system of Ret^{C620R} homozygous mice. To determine the presence of neurons from the enteric nervous system (ENS) of the mice, antibodies specific for neuron-specific enolase (anti-NSE) as a general neuronal marker[27] were used. Microscopic analysis and immunohistochemistry performed with anti-NSE demonstrated that enteric ganglion cells were absent in the stomach, and in the small or large bowel of Ret^{C620R} homozygous animals (Figure 3) although they were present in both wild-type and heterozygous mice. The absence of enteric neurons in the foregut, midgut, and hindgut highlights similarities between these mice and both the Ret- and Gdnf-deficient mice.[7,28] This fact indicates that, at least in this genetic

background, the introduction of the Ret^{C620R} mutation has effects comparable to deleting either Ret or Gdnf.

Kidney formation depends on a succession of interactions that occur between the ureteric bud (UB) and the metanephric mesenchyme. RET is produced in the nephric duct and in the nascent UB, and subsequently its activity is restricted to the tips of the branching bud. Compelling evidence has demonstrated that, consistent with a similar expression pattern of GFRα-1 and GDNF, GDNF is a morphogen and exhibits paracrine activity in the UB. Gdnf-, Gfrα-1-, and Ret-null mice show renal agenesis or have hypoplastic kidneys because of the lack of UB growth, suggesting a crucial role for this receptor in UB development.[29] In line with this, the analysis of the homozygous Ret^{C620R} newborn mice demonstrated agenesis of the kidneys as well as empty bladders (Figure 4). All of the mice lacked both kidneys.

Ret Expression in Ret^{C620R} Homozygous Embryos

Whole-mount immunostaining experiments using an antibody specific for RET were performed in Ret^{C620R} embryos to assess possible abnormalities in the distribution of the Ret^{C620R}-expressing cells. As shown in Figure 5A, consistent with previously reported data,[8] in 10.5 dpc wild-type embryos a Ret-specific signal is observed in a population of cells located ventral to, and apparently in association with, the cervical branches (Figure 5A, arrows). In Ret^{C620R} homozygotes of the same age, no RET staining is visible in these areas, however specific staining is observed to correspond with the fascioacoustic ganglion (Figure 5B). In 11.5 dpc wild-type embryos, two populations of cells are present, a ventrally located one that will probably invade the foregut mesenchyme (Figure 5C, arrows), and a more dorsal group located proximal to the dorsal aorta (Figure 5A, arrows). In 11.5 dpc Ret^{C620R} homozygotes, no Ret staining is visible in these areas indicating that there are no Ret-positive cells contributing to the formation of the ENS. These findings suggested that Ret is crucial for the migration and proliferation of ENS progenitors expressing this receptor tyrosine kinase during embryogenesis.

Reduced Enteric Innervation and Muscle Layer Thickness of the GI Tract in Adult Ret^{C620R} Heterozygous Mice

When comparing heterozygous Ret^{C620R} mice to wild-type counterparts of the same age and sex, no differences in morphological features were found. The animals were the same size and during necroscopies, all of the major organs were removed, weighed, and analyzed. We noted a somewhat variable distribution of histopathological findings that were not related to the genotype but, rather, could be ascribed to the age of the animals (data not shown). To evaluate the number and mesh density of enteric neurons to discern subtle differences between wild-type animals and heterozygotes, the whole GI tract was sectioned and immunohistochemical analysis with NSE antibody was used to detect neurons and their extension along GI tracts (Figure 6A). We evaluated the number of ganglia and neurons for each tract in three different $\times$400 fields. For each section, the ganglia were identified as an aggregation of NSE-positive cells, located either between the smooth muscle layers (myenteric plexus) or between the mucosa and circular smooth muscle layer (submucosal plexus). Within the ganglia, neurons were considered as cells with NSE-positive cytoplasm and hematoxylin-stained nuclei. Quantitative analysis performed according to Sanovic and colleagues,[30] indicated that the numbers of ganglionic cells were reduced in heterozygous animals when compared to wild-type littermates. In particular, male heterozygotes had a lower number of neurons in the stomach, duodenum, jejunum, ileum, cecum (apex and body), and in the colon (Figure 6B). Heterozygote females showed the same features in the duodenum, ileum, cecum (apex and body), and both in the distal and proximal part of the colon (Figure 6C). The size of the ganglion cells was also small in some heterozygous mice (Figure 6A). Taken together these data indicate that there is a general hypoganglionosis in the GI tracts of Ret^{C620R} heterozygous mice.

Together with the observed hypoganglionosis, histological analysis of the muscular layer along the GI tract displayed a reduction in thickness (visible in Figure 6A) that was further evaluated using morphometric analysis on the whole GI tract. At least three images for each tract were evaluated according to the method described by Starck and Rahmaan.[23] In male Ret^{C620R} heterozygous mice the muscular layer of the stomach, duodenum, cecum (apex and body), proximal and distal colon was thinner than that of wild-type mice (Figure 6D). Ret^{C620R} female heterozygotes displayed a reduced muscle layer thickness in the stomach, duodenum, jejunum, cecum (apex), proximal and distal colon (Figure 6E).

Discussion

The occurrence of HSCR in many MEN 2A/FMTC pedigrees is difficult to clarify. Proposed explanations vary based on the cell system used. A decreased cell surface expression of RET,[15,16] an inability to respond to GDNF and to protect RET-expressing cells from apoptosis,[31] or a kinase activity under a threshold otherwise required for cell survival,[14] were all offered as reasons possible for the dual phenotypes associated with mutation of the RET Cys620.

These earlier hypothesis encouraged us to generate an *in vivo* model to facilitate studying the effects of this mutation. Through the introduction of the Cys620Arg substitution in the murine Ret receptor tyrosine kinase, we provide evidence that the mutant *Ret*^{C620R} allele exerts a dramatic loss-of-function effect. All of the homozygous mutant animals die within 12 to 24 hours of birth, exhibit renal agenesis, and lack enteric ganglia along the whole GI tract. Moreover, this knock-in mouse model has sev-

eral features characteristic of HSCR disease. Mice heterozygous for the mutant *Ret*^{C620R} allele display hypoganglionosis of the GI tract.

Previous studies have established the absolute requirements for Ret in the development of the enteric nervous system and kidneys.[7,8,29] The phenotype of

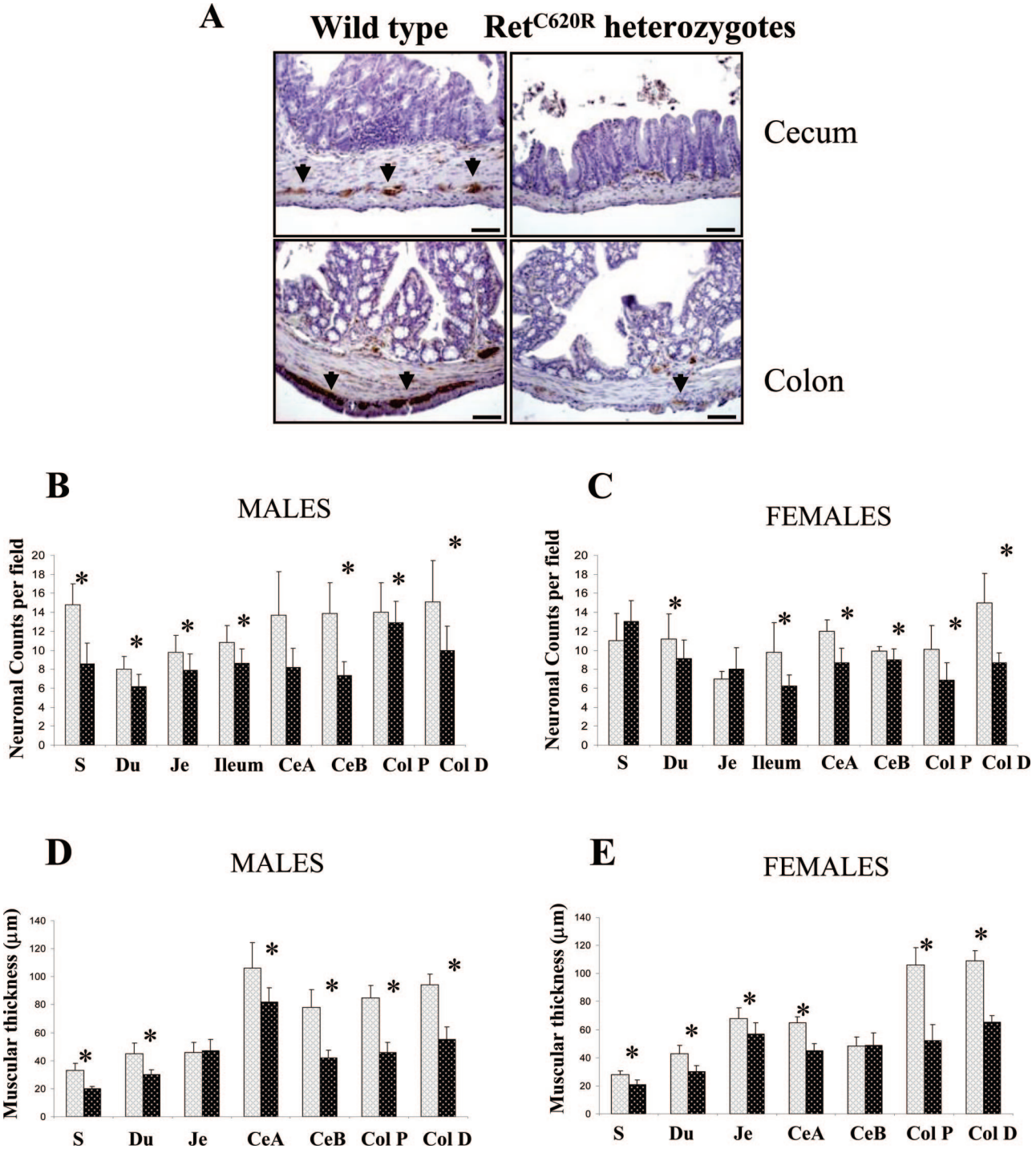

Figure 6. Quantitative analysis of neuronal densities and mucosal thickness along the GI tract. **A:** Immunohistochemical analysis of the enteric nervous system of Ret^{C620R} heterozygous mice with NSE staining that identifies a consistent number of ganglion cells (**arrows**) in the wall of the GI tract of wild-type animals whereas less staining is present in Ret^{C620R} heterozygous mice. The number of neurons, defined as cells with NSE-positive cytoplasm and hematoxylin-stained nuclei, was counted in three ×400 fields in each GI tract in adult wild-type and Ret^{C620} heterozygous male (**B**) and female (**C**) mice. Hypoganglionosis in the GI tract in the Ret^{C620R} heterozygous mice was also associated with a reduction in the thickness of the muscular layer. Muscular thickness of three ×100 fields/mouse in each GI tract was measured. The results of the digital image analysis of muscular thickness along GI tracts in adult wild-type and Ret^{C620} heterozygous male (**D**) and female (**E**) mice are shown. The **arrows** indicate the tracts where a correlation between low muscular thickness and low neuron number was observed. S, stomach; Du, duodenum; Je, jejunum; CeB, cecum (body); CeA, cecum (apex); Col P, proximal colon; Col D, distal colon. Data represent the mean values obtained from 10 mice per group. Error bars indicate the 95% confidence interval. Statistical significance of heterozygous (**filled columns**) versus control wild-type mice (**open columns**) was assessed by two-sided Student's *t*-test (*$P < 0.001$). Scale bars, 50 µm.

Ret^{C620R} homozygous mice showing complete bilateral kidney agenesis and hypoganglionosis along the GI tract is similar to that of Ret-deficient animals indicating that this substitution completely impairs Ret function during development. In addition, mice expressing null mutations in either Gdnf or Gfrα-1 also die shortly after birth and lack the ENS in the bowel.[4,26,32] These knockout mice show renal agenesis or have hypoplastic kidneys because they lack UB growth.[4,28,32]

Our results suggest that the *Ret*^{C620R} gene encodes a 140-kd protein that was shown to be mislocalized in different cell systems (Figure 2C and Robertson and colleagues[24]) and in primary culture obtained from Ret^{C620R} homozygous brains (Figure 2B). It is therefore likely that in our mouse model the Ret^{C620R} substitution, rendering the receptor unable to localize correctly at the cell surface, impairs the formation of an essential complex with GDNF and GFRα-1 required for ENS and kidney development.[28,29,32] The reduced innervation along the GI tract of Ret^{C620R} heterozygous mice might be explained by the fact that Ret activation by GDNF is not only essential for formation of the ENS, but GDNF availability also determines the total number of enteric neurons in both the colon and the small intestine.[33] Enteric neuron number is determined by controlled cell proliferation rather than by apoptosis in wild-type mice and is dependent on an adequate amount of trophic factors.[33] Gene dosage effects, such as the reduction in neuron number seen in Gdnf$^{+/-}$ mice[34] suggest that quantity and quality of neurotrophic factor signaling can limit neuronal survival or proliferation.[33] Interestingly, Ret mutations that cause HSCR disease in humans are inactivating mutations penetrant in the heterozygous state. The partial reduction in enteric neuron size and neuronal fiber counts observed in Ret$^{+/-}$ mice[33] and the more substantial one observed in our mouse model, might imply that in humans ENS precursors have more limiting Ret expression than the corresponding murine cells. Recent data also suggest that in humans, the penetrance of Ret mutations may depend on the presence of second site modifiers that could affect Ret expression.[35]

It has been nicely shown that HSCR disease is caused by defects in neural crest stem cell (NCSC) function.[36] In the esophagus of E13.5 Ret-null mice, a partially detectable reduction in the number of NCSCs has been described whereas the effect was more striking in the stomach and intestine of E13.5 Ret-null mice, indicating that few stem cells could migrate beyond the esophagus thus explaining the absence of enteric ganglia in the distal stomach and intestine of Ret-deficient animals. Moreover, Gdnf did not affect NCSCs survival or proliferation but the reduction in NCSC frequency in the stomach and intestine is likely caused by a defect in migration.[36] Most neural crest cells that colonize the gut are Ret-dependent and derive from the vagal neural crest, whereas a minority of neural crest cells that colonize the esophagus are Ret-independent and derive from the trunk neural crest.[37] RET signaling therefore is required for the colonization of the gut by NCSCs.[36] This is consistent with reports that Gdnf is expressed in the gut in advance of migrating neural crest cells thereby acting as a chemoattractant for neural crest cells in culture[38,39] in which GDNF/RET signaling is required for invasion of the foregut and the subsequent migration of enteric NC cells along the length of the bowel.[39] In E10.5 and E11.5 Ret^{C620R} homozygous mice, no Ret-expressing cells invading the foregut were detected as is the case in normal mice. These findings would suggest that the migration of Ret^{C620R}-expressing cells is impaired but future studies will be necessary to clarify whether this Ret mutation impairs most vagal-derived NCSC migration as in the case of Ret-null mice.[36] Still, the HSCR phenotype outlined in Ret^{C620R} mice seems to reflect defects in the ability of Ret-expressing cells to migrate toward defined stimuli necessary for invasion of the bowel by neural crest precursor cells. Expression of key guidance cues and activation of receptors on the cell surface are necessary for the generation of directional cell migration.[40,41] On the other hand, we cannot exclude the possibility that these cells die before the colonization of the gut.

To our surprise, none of our mice developed significant dysfunctions in the thyroid gland (data not shown) even when maintained up to 2 years. When monitoring calcitonin serum levels of heterozygous mice we were never able to find increments (data not shown). This together with careful analysis of the thyroid and adrenal glands, tissues in which humans with MEN 2A typically develop cancer, indicates absence of C-cell hyperplasia and neoplasia. It seems possible that the oncogenic signals triggered from physiological levels of the Ret^{C620R} mutant are insufficient to drive tumor formation. Alternatively, modifier genes may exist that must also be expressed in addition to activated Ret for the development of MTC. Moreover these modifier genes may or may not be present in any particular strain of inbred mouse. Recent findings by Cranston and Ponder,[42] demonstrated that in a Ret transgenic mouse model the proportion of mice with bilateral MTC was different depending on the strain background in which the transgene was expressed therefore raising the possibility of modifier effects attributable to genetic background. In light of this it would be interesting to use different genetic backgrounds to assess susceptibility to both HSCR and MTC in our Ret^{C620R} knock-in mouse model.

In conclusion, in this study we elucidated the *in vivo* role of the signaling via Ret^{C620} by targeted mutagenesis of the Ret receptor tyrosine kinase. This signaling appeared to play a crucial role in the migration and/or proliferation of ENS progenitors because the neuron number and distribution in the intestine of Ret^{C620R} heterozygous mice were markedly reduced and absent in Ret^{C620R} homozygous mice. Moreover, signaling via Ret^{C620} was required for kidney formation. In addition to facilitating the elucidation of the signal transduction events triggered by this RET mutant, this mouse model provides the opportunity to explore further the pathophysiological manifestation of HSCR disease induced by this mutation. This knock-in mouse model could also represent a very interesting system for the study and testing of new therapeutic approaches for the treatment of HSCR disease such as neural stem cell transplantation to reconstruct the innnervation of the GI tracts.

Acknowledgments

We thank Arlette Franchi for ES cell assistance; Ted Saunders and the staff of the Gene Targeting Facility at the Babraham Institute, Cambridge, UK, for blastocyst injections; Gaetano Mellillo of the animal facility at the Istituto Tumori, Milano, Italy, for assistance in mouse husbandry; Ken Jones for technical assistance in constructing the targeting vector; Giacomo Manenti and Debora Degl'Innocenti for helpful discussion during manuscript preparation; and Cristina Mazzadi for secretarial help.

References

1. Takahashi M, Ritz J, Cooper GM: Activation of a novel human transforming gene, ret, by DNA rearrangement. Cell 1985, 42:581–588
2. Takahashi M, Buma Y, Iwamoto T, Inaguma Y, Ikeda H, Hiai H: Cloning and expression of the ret proto-oncogene encoding a tyrosine kinase with two potential transmembrane domains. Oncogene 1988, 3:571–578
3. Taraviras S, Pachnis V: Development of the mammalian enteric nervous system. Curr Opin Genet Dev 1999, 9:321–327
4. Baloh RH, Enomoto H, Johnson Jr EM, Milbrandt J: The GDNF family ligands and receptors—implications for neural development. Curr Opin Neurobiol 2000, 10:103–110
5. Jhiang SM: The RET proto-oncogene in human cancers. Oncogene 2000, 19:5590–5597
6. Parisi MA, Kapur RP: Genetics of Hirschsprung disease. Curr Opin Pediatr 2000, 12:610–617
7. Schuchardt A, D'Agati V, Larsson-Blomberg L, Costantini F, Pachnis V: Defects in the kidney and enteric nervous system of mice lacking the tyrosine kinase receptor Ret. Nature 1994, 367:380–383
8. Durbec PL, Larsson-Blomberg LB, Schuchardt A, Costantini F, Pachnis V: Common origin and developmental dependence on c-ret of subsets of enteric and sympathetic neuroblasts. Development 1996, 122:349–358
9. Pachnis V, Mankoo B, Costantini F: Expression of the c-ret proto-oncogene during mouse embryogenesis. Development 1993, 119:1005–1017
10. Tsuzuki T, Takahashi M, Asai N, Iwashita T, Matsuyama M, Asai J: Spatial and temporal expression of the ret proto-oncogene product in embryonic, infant and adult rat tissues. Oncogene 1995, 10:191–198
11. Mulligan LM, Eng C, Attie T, Lyonnet S, Marsh DJ, Hyland VJ, Robinson BG, Frilling A, Verellen-Dumoulin C, Safar A: Diverse phenotypes associated with exon 10 mutations of the RET proto-oncogene. Hum Mol Genet 1994, 3:2163–2167
12. Hansford JR, Mulligan LM: Multiple endocrine neoplasia type 2 and RET: from neoplasia to neurogenesis. J Med Genet 2000, 37:817–827
13. Decker RA, Peacock ML, Watson P: Hirschsprung disease in MEN 2A: increased spectrum of RET exon 10 genotypes and strong genotype-phenotype correlation. Hum Mol Genet 1998, 7:129–134
14. Takahashi M, Iwashita T, Santoro M, Lyonnet S, Lenoir GM, Billaud M: Co-segregation of MEN2 and Hirschsprung's disease: the same mutation of RET with both gain and loss-of-function? Hum Mutat 1999, 13:331–336
15. Chappuis-Flament S, Pasini A, De Vita G, Segouffin-Cariou C, Fusco A, Attie T, Lenoir GM, Santoro M, Billaud M: Dual effect on the RET receptor of MEN 2 mutations effecting specific extracytoplasmic cysteines. Oncogene 1998, 17:2851–2861
16. Ito S, Iwashita T, Asai N, Murakami H, Iwata Y, Sobue G, Takahashi M: Biological properties of Ret with cysteine mutations correlate with multiple endocrine neoplasia type 2A, familial medullary thyroid carcinoma, and Hirschsprung's disease phenotype. Cancer Res 1997, 57:2870–2872
17. Carlomagno F, Salvatore G, Cirafici AM, De Vita G, Melillo RM, de Franciscis V, Billaud M, Fusco A, Santoro M: The different RET-activating capability of mutations of cysteine 620 or cysteine 634 correlates with the multiple endocrine neoplasia type 2 disease phenotype. Cancer Res 1997, 57:391–395
18. Asai N, Iwashita T, Matsuyama M, Takahashi M: Mechanism of activation of the ret proto-oncogene by multiple endocrine neoplasia 2A mutations. Mol Cell Biol 1995, 15:1613–1619
19. Santoro M, Carlomagno F, Romano A, Bottaro DP, Dathan NA, Grieco M, Fusco A, Vecchio G, Matoskova B, Kraus MH, Di Fiore PP: Activation of RET as a dominant transforming gene by germline mutations of MEN2A and MEN2B. Science 1995, 267:381–383
20. Borrello MG, Smith DP, Pasini B, Bongarzone I, Greco A, Lorenzo MJ, Arighi E, Miranda C, Eng C, Alberti L, Bocciardi R, Mondellini P, Scopsi L, Romeo G, Ponder BAJ, Pierotti MA: RET activation by germline MEN2A and MEN2B mutations. Oncogene 1995, 11:2419–2427
21. Greenfield L, Bjorn MJ, Horn G, Fong D, Buck GA, Collier RJ, Kaplan DA: Nucleotide sequence of the structural gene for diphtheria toxin carried by corynebacteriophage beta. Proc Natl Acad Sci USA 1983, 80:6853–6857
22. Taniguchi M, Sanbo M, Watanabe S, Naruse I, Mishina M, Yagi T: Efficient production of Cre-mediated site-directed recombinants through the utilization of the puromycin resistance gene, pac: a transient gene-integration marker for ES cells. Nucleic Acids Res 1998, 15:679–680
23. Starck JM, Rahmaan GH: Phenotypic flexibility of structure and function of digestive system of Japanese quail. J Exp Biol 2003, 206:1887–1897
24. Robertson E, Bradley A, Kuehn M, Evans M: Germ-line transmission of genes introduced into cultured pluripotential cells by retroviral vector. Nature 1986, 323:445–448
25. Arighi E, Popsueva A, Degl'Innocenti D, Borrello MG, Carniti C, Perala NM, Pierotti MA, Sariola H: Biological effects of the dual phenotypic Janus mutation of RET cosegregating with both multiple endocrine neoplasia type 2 and Hirschsprung's disease. Mol Endocrinol 2004, 18:1004–1017
26. Takahashi M, Asai N, Iwashita T, Isomura T, Miyazaki K, Matsuyama M: Characterization of the ret protooncogene products expressed in mouse L cells. Oncogene 1003, 8:2925–2929
27. Neunlist M, Aubert P, Toquet C, Oreshkova T, Barouk J, Lehur PA, Schemann M, Galmiche JP: Changes in chemical coding of myenteric neurones in ulcerative colitis. Gut 2003, 52:84–89
28. Moore MW, Klein RD, Farinas I, Sauer H, Armanini M, Phillips H, Reichardt LF, Ryan AM, Carver-Moore K, Rosenthal A: Renal and neuronal abnormalities in mice lacking GDNF. Nature 1996, 382:76–79
29. Schuchardt A, D'Agati V, Pachnis V, Costantini F: Renal agenesis and hypodysplasia in ret-k-mutant mice result from defects in ureteric bud development. Development 1996, 122:1919–1929
30. Sanovic S, Lamb DP, Blennerhassett MG: Damage to the enteric nervous system in experimental colitis. Am J Pathol 1999, 155:1051–1057
31. Mograbi B, Bocciardi R, Bourget I, Juhel T, Farahi-Far D, Romeo G, Ceccherini I, Rossi B: The sensitivity of activated Cys Ret mutants to glial cell line-derived neurotrophic factor is mandatory to rescue neuroectodermic cells from apoptosis. Mol Cell Biol 2001, 21:6719–6730
32. Airaksinen MS, Titievsky A, Saarma M: GDNF family neurotrophic factor signaling: four masters, one servant? Mol Cell Neurosci 1999, 13:313–325
33. Gianino S, Grider JR, Cresswell J, Enomoto H, Heuckeroth RO: GDNF availability determines enteric neuron number by controlling precursor proliferation. Development 2003, 130:2187–2198
34. Shen L, Pichel J, Mayeli T, Sariola H, Lu B, Westphal H: Gdnf haploinsufficiency causes Hirschsprung-like intestinal obstruction and early-onset lethality in mice. Am J Hum Genet 2002, 70:435–447
35. Gabriel SB, Salomon R, Pelet A, Angrist M, Amiel J, Fornage M, Attie-Bitach T, Olson JM, Hofstra R, Buys C Steffann J, Munnich A, Lyonnet S, Chakravarti A: Segregation at three loci explains familial and population risk in Hirschsprung disease. Nat Genet 2002, 31:89–93
36. Iwashita T, Kruger GM, Pardal R, Kiel MJ, Morrison SJ: Hirschsprung disease is linked to defects in neural crest stem cell function. Science 2003, 301:972–976
37. Durbec PL, Larsson-Blomberg LB, Schuchardt A, Constantini F, Pachnis V: Common origin and developmental dependence on c-ret

of subsets of enteric and sympathetic neuroblasts. Development 1996, 122:349–358
38. Young HM, Hearn CJ, Farlie PG, Canty AJ, Thomas PQ, Newgreen DF: GDNF is a chemoattractant for enteric neural cells. Dev Biol 2001, 229:503–516
39. Natarajan D, Marcos-Gutierrez C, Pachnis V, de Graaff E: Requirement of signalling by receptor tyrosine kinase RET for the direct migration of enteric nervous system progenitor cells during mammalian embryogenesis. Development 2002, 129:5151–5160
40. Duchek P, Rorth P: Guidance of cell migration by EGF receptor signaling during Drosophila oogenesis. Science 2001, 291:131–133
41. Duchek P, Somogyi K, Jekely G, Beccari S, Rorth P: Guidance of cell migration by the drosophila PDGF/VEGF receptor. Cell 2001, 107:17–26
42. Cranston AN, Ponder BAJ: Modulation of medullary thyroid carcinoma penetrance suggests the presence of modifier genes in a RET transgenic mouse model. Cancer Res 2003, 63: 4777–4780